Efficient Excitation Signals for the Fast Impedance Spectroscopy

J. Ojarand[1], M. Min[2]
[1]ELIKO Competence Centre,
Maealuse 2/1, 12618 Tallinn, Estonia
[2]Th. J. Seebeck Department of Electronics, Tallinn University of Technology,
Ehitajate tee 5, 19086 Tallinn, Estonia
jaan.ojarand@eliko.ee

Abstract—**This paper deals with finding the highly efficient multifrequency excitation waveforms for fast bioimpedance spectroscopy. However, the solutions described here could be useful also in other fields of impedance spectroscopy. Theoretically, the useful excitation power of optimized binary multifrequency signals (BMS) exceeds the power of comparable multisine waveforms. However, part of power of the BMS waveforms is spread between higher harmonics of the wanted frequency components. In practical use of voltage excitation, the higher harmonics complicate the signal processing and produce current spikes passing through the capacitive elements of the impedance to be measured. In the paper, we show that the excitation power of well-optimized multisine with decaying amplitudes comes close to the power of comparable binary waveform while reducing the problems caused by unwanted frequency components. This allows simpler signal processing. Besides, we also show that the overall efficiency of using of the multisine excitation in impedance measurement becomes even higher efficient than the BMS in practice, despite the fact that the power of binary waveforms is the highest.**

Index Terms—**Signal design, binary multifrequency signal, multisine signal, impedance measurement, bioimpedance spectroscopy.**

I. INTRODUCTION

Electrical bioimpedance spectra are widely used to characterize the structure of tissues and cell cultures [1]. In cases where the properties of the object are changing in time (e.g. pumping heart muscle) or the objects move as cells in a microfluidic channel, the frequency range of interest must be covered in a short timeframe. Therefore, the energy of the excitation signal must be spread between multiple frequencies during this timeframe.

Concurrently, such an important criterion of the efficiency of measurements – the signal-to-noise ratio (SNR) of measured response signal – is proportional to the square of root-mean-square (RMS) values of frequency components of the excitation signal. Unfortunately, in bioimpedance measurements the SNR cannot be improved by increasing the overall amplitude of the excitation signal since it is limited to much lower values [2] than the signal ranges and power supply voltages of non-biologic measurement devices. There are still two main possibilities for improving the SNR of bioimpedance measurements by optimizing the properties of the wideband excitation signals.

At first, minimizing the ratio of signal's peak value in respect to its RMS value, called as a crest-factor (CF). Recently a novel CF minimization method for multisine waveform was proposed in [3], which gives the CF below the value corresponding to a single sine wave (CF = $\sqrt{2}$), if the same level frequency components are distributed equally. The smallest crest factor (CF = 1) have the waveforms of binary multifrequency signals (BMS).Comparison of RMS values of the frequency components of different wideband excitation signals is given in [4]. The significance of lower CF values is explained hereinafter.

Secondly, the excitation waveforms with spectrally sparse distribution of frequency components are the most preferable. Bioimpedance spectra have a smooth shape and tendency to decrease at higher frequencies [1]–[4] as illustrated in Fig. 1. More accurate electrical models include also constant phase elements (CPE) acting at lower frequencies (-dispersion range), but not changing the situation in -dispersion range of interest covering 2–3 decades within the kHz to MHz band [1]. It is obvious that the spectral components with sparse frequencies attain higher RMS values in the composite signals with limited amplitudes.

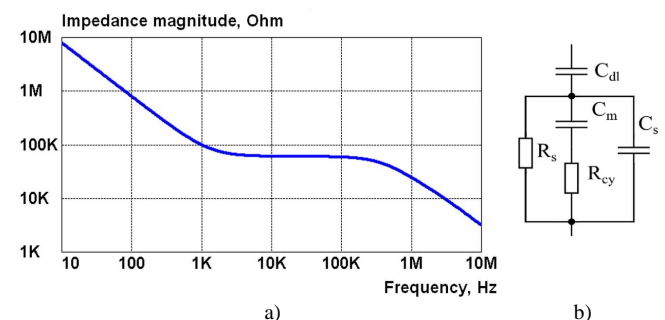A simplified architecture of the bioimpedance spectroscopy system is shown in Fig. 2.

Fig. 1. A magnitude spectrum of the impedance of a single cell in saline suspension (a) using simplified electrical model (b) with C_{dl} = 2nF, C_m = 1 pF, C_s = 5pF, R_s = 60 k and R_{cy} = 100 k .
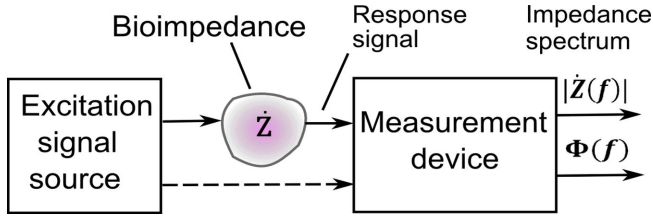
Fig. 2. A simplified architecture of the spectroscopy system designed for measurement of complex bioimpedance , with magnitude (amplitude) spectrum | (f)| and phase spectrum (f) as the functions of frequency f.

More exactly, to measure unknown impedance, we can choose one of two approaches: either we apply a known voltage excitation across the object and measure the current flowing through, or we inject a known current excitation into that object and measure the voltage response across it. We can also measure both, current and voltage, simultaneously. The last method is preferable, if the excitation source is not stable. This situation is typical for current sources at very high frequencies since their output impedance decreases because of stray capacitances and degradation of the performance of electronic components [5].

The accuracy of fitting of parameters of the electrical model depends also on the number of frequency components [4], but this topic is out of scope of the present paper.

II.   ADAPTING THE SHAPE OF SPECTRUM

A current mode excitation with pre-emphasized rising power spectrum at higher frequencies compensates a reducing response of impedance in the high frequency range beginning from 100 kHz in Fig. 1(a).

The rise of impedance in lower frequency area is mostly caused by polarization of electrodes (double layer effect) and usually does not give much information about the properties of biological objects. Therefore, this part of the spectrum can be excluded, paying attention to the avoidance of possible declination in parameter fitting [6] in the electrical model (Fig. 3(b)). There are at least two possibilities for obtaining the rising spectrum of current excitation at higher frequencies. As shown in [7], the BMS waveform can be designed with such spectrum, but the mean RMS value of excitation will be less than in the case of flat spectrum. The similar disadvantage characterizes also multisine waveforms though the amplitudes of signal components are freely selectable – the CF increases almost proportionally to the highest amplitude of the spectral components. This is a common disadvantage of using the current mode excitation in bioimpedance spectroscopy.

The use of a voltage source for generating a simple excitation of binary rectangular waveform (Fig. 3) is proposed as a robust and efficient solution for covering a decaying part of the impedance spectrum [2]. One benefit of using a voltage source is that only the current response could be measured since it is relatively easy to generate the stable voltage excitation in a required frequency range. Furthermore, the decaying amplitude spectrum of regular rectangular voltage (Fig. 3(a)) fits well with the also decaying spectrum of the impedance to be measured (Fig.1). However, this solution has an essential drawback described in the next section – the current response will obtain the high-peak waveform with inadmissibly high CF.

III.   VOLTAGE SOURCE AND CURRENT SPIKES

A.   Spikes of the Response Current and Crest Factor

A binary waveform excitation (Fig. 3(a)) produces large current spikes due to re-charging of the capacitance C_s in the impedance model (Fig. 3(b)), as illustrated in Fig. 4(a). Though a series resistor R_a allows limit the peaks, the most of the input range of the measurement device remains still occupied by the spike like current response.
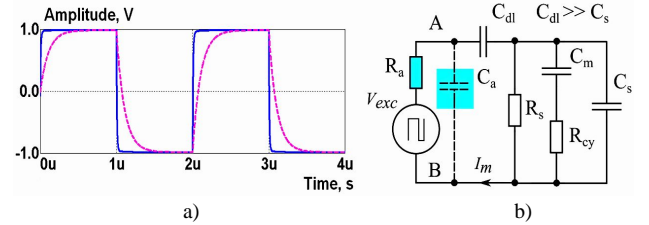

Fig. 3. Waveforms (a) of the voltage between the points A and B (b), when $R_a = 1$ k , $C_a = 2$ pF (solid line), and when $R_a = 1$ k , $C_a = 100$ pF (dashed line). Values of other elements are the same as shown in Fig. 1.

Artificial increasing of the stray capacitance C_a in Fig. 3(b) allows further suppressing of current spikes (Fig. 4(c)). However, as shown in Fig. 4(d), the RMS values of the useful spectral components in the response current are decreasing significantly.
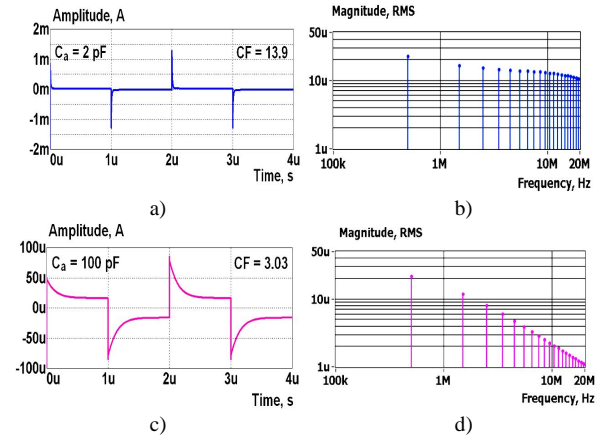

Fig. 4. Waveforms (a) and (c) and the corresponding spectra (b) and (d) of the response current I_m in case shown in Fig. 3. CF denotes the crest factor.

Note that there is also a small stray capacitance (around 0.2 pF) in parallel with R_a, which is not shown in Fig. 3(b). In turn, this capacitance increases the current spikes. However, the limited speed of changes in the voltage excitation produces the opposite effect, e.g., if the duration of voltage frontline is ≥ 2 ns, the impact of this stray capacitance is negligible.

Despite the fact that the CF of square wave excitation voltage is minimal, the CF of the response current becomes high (Fig. 4(a) and Fig. 4(c)). The CF [8] is expressed in (1), wherein T denotes the observation time of the voltage or current signal, $s(t)$, and a divisor of the equation represents the RMS value of the signal.

$$CF(s) = \frac{\underset{t \in [0,T]}{Max} |s(t)|}{\sqrt{\dfrac{1}{T} \int_0^T s^2(t)dt}}.$$

(1)

B. Influence of the CF on SNR

The SNR is expressed through the ratio of signal and noise power P_{sig}/P_{noise}, while power P is equal to the square of RMS value. Usually we expect a digital processing of signals. The power of quantization noise of an ideal n-bit analog-to-digital converter (ADC) diminishes approximately by a factor of 4 for every additional bit [9]. According to (1), the RMS level of the signal with given maximum amplitude is decreasing proportionally to its CF, and P_{sig} decreases by factor of 4 if the CF increases twice. It follows that the required resolution of the ADC in bits is proportional to the CF of the signal to keep the same SNR of analog-to-digital conversion.

The quantization noise is not only and neither the most important factor in determining the SNR. The noise of electronic components becomes more important as the required resolution is rising. For example, the noise of the reference voltage could have a higher impact, than the quantization noise of high resolution ADCs. Influence of external disturbances and the deterioration of behaviour of electronic circuits at high frequencies can be viewed as noise as well [9]. In addition, the jitter of clock signals transfers also as an equivalent amplitude noise.

In case of uncorrelated noise sources and the maximum possible amplitude A_{max} of the signal in (1), the SNR expresses in dB as follows in (2), in which $S_{noise(RMS)}$ denotes a sum of all the noise components

$$SNR_{DB} = 10 \log_{10}(P_{sig} / P_{noise}) =$$
$$= 10 \log_{10}(A_{max}^2 / CF^2 \cdot S_{noise(RMS)}^2) =$$
$$= 20 \log_{10}(A_{max} / CF \cdot S_{noise(RMS)}). \quad (2)$$

The SNR is inversely proportional to CF (2), but in the case of wideband excitation, there is another important factor to consider. The RMS value of the excitation signal represents the cumulative value of all its components. In case of discrete set of frequencies it expresses as

$$S_{sig(RMS)} = \sqrt{\sum_1^k (S_{sig(RMS)}(i))^2}, \quad (3)$$

where i is the index of relative frequency of components and k is the number of frequency components. Assuming that the noise power density is uniform in the frequency range of interest, the SNR of spectral measurement depends on the RMS of spectral components. If the spectrum has a decaying form as in Fig. 4d, the SNR also decays with frequency. In this case, the CF characterizes only a mean SNR value.

One more important drawback of high CF is the higher probability of saturation of the measurement channel, which may substantially distort the measurement results.

C. Solutions for Reducing the CF of Response Current

A simple out-filtering of useless higher frequency components in the rectangular signal improves the CF, but the concurrent decrease of amplitudes of the useful signal components (Fig. 4(d)) makes this almost worthless.

Another solution, the shaping of square wave excitation so that it would have a smooth shape and moderate steepness of

frontline, seems reasonable. This hypothesis was tested by modifying the square waveform with a sigmoid function

$$Sigm(t) = \pm 1 / (1 + e^{\pm xt}). \quad (4)$$

Variable x in (4) determines the frontline steepness of a pulse waveform. The results are illustrated in Fig. 5. The crest factor of the current response, $CF_r = 3.58$, is significantly better (smaller), than in the case of original square wave excitation (Fig. 4(a)), but the amplitude spectrum decays fast above 5 MHz. The crest factor of the excitation waveform $CF_e = 1.04$ maintains its low level.

Higher-order filtering and a waveform shaping could somewhat improve the CF and spectrum of the response current, but still two serious disadvantages remain. First, the measurement of the excitation signal is required in the most cases, since it is hard to guarantee accurate and stable spectra after the filtering or shaping. Secondly, a waveform shaping must be done in real time, which requires additional hardware resources.
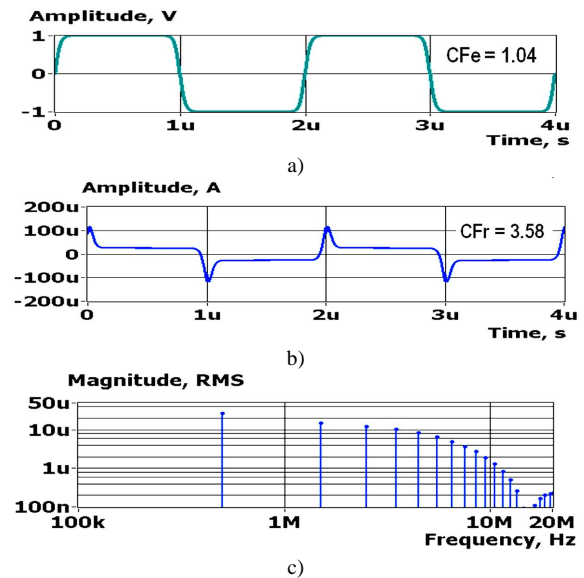

Fig. 5. Waveforms of voltage excitation (a), current response (b) and the spectrum of current response (c) at $R_a = 1$ k , $C_a = 2$ pF and $x = 100$.

An alternative solution to overcome the problems described above is proposed in the next section.

IV. SUBSTITUTING A SQUARE WAVE WITH A MULTISINE

A. Composing a Square Wave Signal

It is well known that a periodic signal can be composed of the sum of harmonically related cosine and sine waves of different amplitudes (Fourier series). In particular, we can build a square wave summing up infinite number of sine wave odd harmonics, if the amplitudes of these harmonic components with $i = 1, 3, 5, 7, \ldots, \infty$ follow the rule

$$A(i) = 1 / i, \quad (5)$$

in which i is an index of the relative frequency. This decaying form of amplitude spectrum suits well for using of a voltage excitation source. If the unit amplitude square wave is desired, the amplitudes $A(i)$ in (5) must be

multiplied by 4/ .

When the number of frequency components is finite, the shape of the waveform somewhat differs from the square wave. At the same time, the limited number of components is very practical advantage because of absence of unwanted higher harmonics in the excitation signal – only the frequency components needed for composing the required multisine waveform are present in the spectrum.
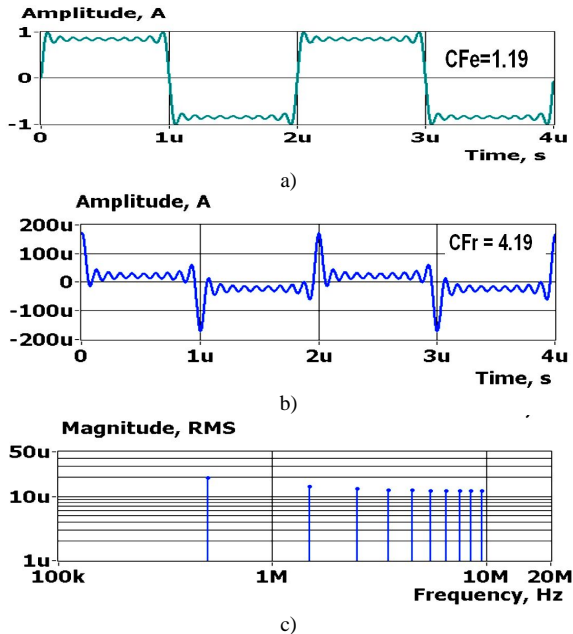

a)

b)

c)

Fig. 6. Waveforms of voltage excitation (a) and current response (b), and the spectrum of response current (c) at $R_a = 1$, $C_a = 2$ pF. The relative frequencies in the spectrum (c) are: $i = 1, 3, 5, 7, 9, 11, 13, 15, 17$ and 19.
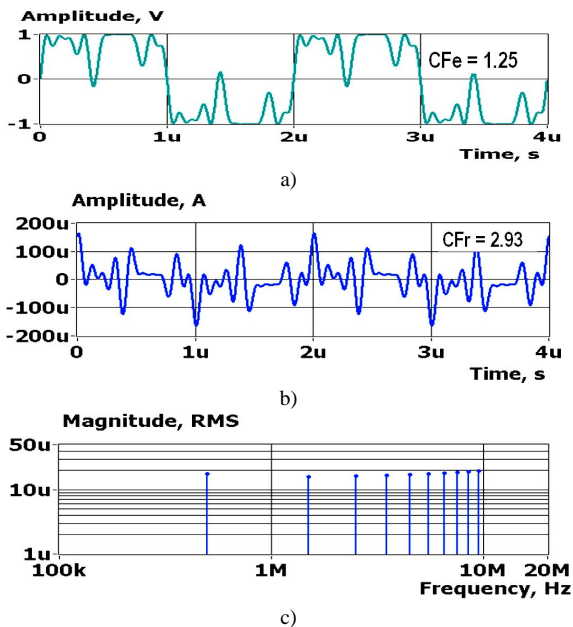

a)

b)

c)

Fig. 7. Waveforms of voltage excitation (a) and current response (b), and the spectrum of response current (c) at $R_a = 1$, $C_a = 2$ pF. The relative frequencies in the spectrum (c) are: $i = 1, 3, 5, 7, 9, 11, 13, 15, 17$ and 19.

In Fig. 6, a case with 10 sine wave components is illustrated. The components have the initial phases $(i) = 0$ and amplitudes $V(i) = 1/i$. Relative frequencies were multiplied by 500×10^3 to get the same frequencies as in previous examples. The CF of this multisine waveform is 1.19, which is below the CF of a single sine wave. It means

that the amplitude of the composite signal (sum of sine waves) is less than 1V. To allow comparison of spectra with other ones, the amplitude of the multisine excitation was normalized to 1V. Amplitudes of the components of normalized multisine excitation $V(i)^*$ can be calculated as

$$V(i)^* = V(i) \sqrt{2} / CF. \qquad (6)$$

The CF_r of the current response is 4.19 and the spectrum is slightly decaying (Fig. 6(c)). Optimizing of initial phases (i) of components using a method given in [3] reduces the CF_e of excitation to 1.14, and the CF_r of the response current to 3.99. However, this improvement gives rise of the RMS value only 3.8 %, and the spectrum remains decaying.

To obtain better results, the rate of decaying the excitation voltage amplitudes must be decreased. In Fig. 7, another waveform of 10 sine wave components is given, where the amplitudes of the components $V(i) = 1/I$ at $= 0.8$, and the initial phases of components are optimized as in [3].

B. Sparse Frequency Distribution

To cover a wider frequency range, sparse distribution of frequencies, e.g. a quasi-logarithmic one, is reasonable. In this case, a small "square wave" appears on top of the main waveform as illustrated in Fig. 8(a).
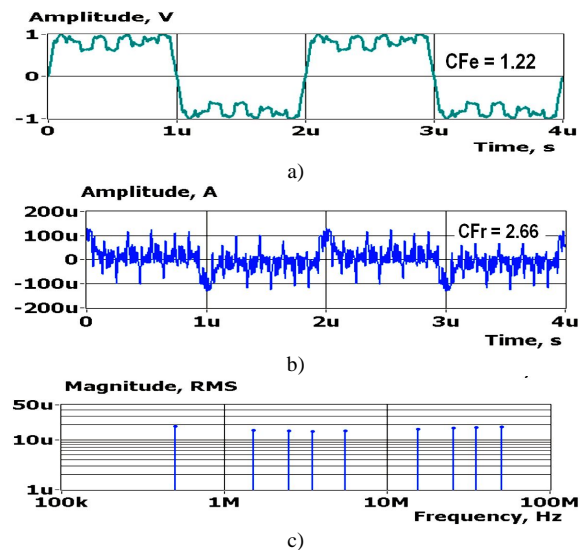

a)

b)

c)

Fig. 8. Waveforms of voltage excitation (a) and current response (b), and the spectrum of response current (c) at $R_a = 1$, $C_a = 2$ pF. The relative frequencies in the spectrum (c) are: $i = 1, 3, 5, 7, 11, 31, 51, 71$ and 101.

The amplitudes of the sine wave components are decaying as $V(i) = 1/i^{0.9}$ and the initial phases were optimized using the method described in [3]. RMS values of the response current spectra in a wider frequency range (from 500 kHz to 50.1 MHz) are almost the same as in the previous example, but the CF_r of the response current is near to 10 % lesser.

C. Stability of Spectra

Note that in all the examples of using multisine waveform a low value series resistor R_a (1) was used to represent the worst situation in respect of current spikes. Actual voltage sources may have larger output resistance. This will also influence the spectra of the excitation signal between the points A and B (Fig. 3(b)).
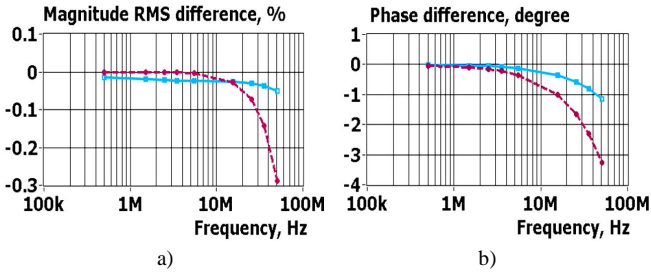
Fig. 9. Deviations of the magnitude (a) and phase (b) spectra due to switching of R_a from 1   to 10   at C_a = 2 pF (solid line), and due to switching of C_a from 2 pF to 20 pF (dashed line) at R_a =10   , see Fig. 3(b).

Dependence of the amplitude and phase spectra on changes of R_a and C_a was tested with a wideband excitation signal given in Fig.8. Differences in the spectra are shown in Fig. 9.

V. Discussion

A. SNR of Measurements When Using a Voltage Source

In general, the SNR at impedance measurement depends on the SNR of both voltage and current measurements. In the particular case of using a voltage excitation with known and stable spectra, only the SNR of the response current measurement remains. However, the crest factors of both, the excitation voltage and current response waveforms still affect the SNR of measurements. For a given (limited) maximum amplitude of the multisine excitation, its RMS value is inversely proportional to CF_e in accordance with (1). The same is true for each component of multisine. Since the RMS values of the response signal depend directly on the excitation signal RMS values, the SNR of impedance measurement for a given maximum peak value of the response current I_{max} can be expressed using (1) and (2)

$$SNR_{DB} = 20\log_{10}\left(\frac{|I_{max}|}{CF_e \cdot CF_r \cdot I_{noise(RMS)}}\right) =$$

$$= 20\log_{10}\left(\frac{I_{resp(RMS)}}{CF_e \cdot I_{noise(RMS)}}\right). \quad (7)$$

$I_{resp(RMS)}$ is the overall RMS value of the response current. It may be concluded that, in case of limited amplitude of the excitation voltage, its crest factor CF_e affects the SNR of impedance measurements in the same rate as the CF_r of the response current. However, if it is possible to increase the amplitude of the excitation voltage and a corresponding increase of I_{max} is allowed, the SNR of measurements will be improved as well.

An example: a multisine with 10 components covering the frequency range from 500 kHz to 9.5 MHz (Fig. 7) provides almost flat spectrum of the response current with RMS level between 16 µA to19 µA and the product of crest factors $CF_e \times CF_r$ = 3.7. A binary square wave (Fig. 3(a)) with the same distribution of frequencies provides a slightly decaying spectrum of the response current between 13 µA to 23 µA (Fig. 4(b)) and the product of crest factors is as high as 14. That is, the SNR of measurements with a multisine excitation is near to 4 times better in this particular case.

B. Covering the Frequency Areas of Impedance Spectra

As shown in Section IV, the decaying part of the magnitude spectrum can be effectively covered with a multisine excitation with properly chosen decay rate   of amplitudes and optimal initial phases   (*i*). To obtain almost flat spectrum of the response signal the first excitation frequency in the amplitude spectrum should be placed on the knee of the impedance spectrum curve (about 300 kHz in Fig 1(a)).

The excitation waveform containing two separate parts proposed in [2] allows maximizing of the RMS level of the response signal also in a flat part of the impedance spectrum. This solution is applicable with multisine waveforms, as well.

Using of multisine with 10 equally spaced frequency components i = 1, 2, 3, …, 10 is illustrated in Fig. 10.
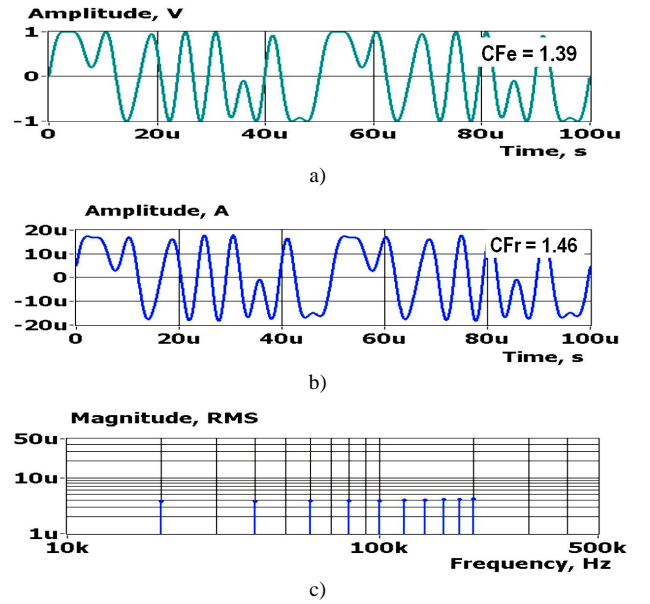

Fig. 10. Waveforms of the voltage excitation (a), the current response (b) and the response current spectrum (c) at relative frequencies i = 1, 2, 3, 4, 5, 6, 7, 8, 9, 10. R_a = 1   and C_a = 2 pF.

The RMS level of the response current is lower in comparison with decaying impedance spectrum (Fig. 7). However, the level of the excitation voltage can be increased since the both crest factors are low. The product $CF_e \times CF_r$ = 2.03, which is less than the product of crest factors (3.25) of signals, shown in Fig. 7. Equation (7) gives the basis to conclude that, in case of equal I_{max}, the SNR of impedance measurements in the flat spectrum area is higher, than in the decaying spectrum area.

A sparser distribution of frequency components, e.g. binary logarithmic one with i = 1, 2, 4, 8, 16, 32 may be also used for measurement the flat area of the spectrum. In this case, typical values of CF_e = 2.0 and CF_r = 2.1 are met, which provides the value of 4.2 for the product of crest factors. However, the frequency range is also wider than in the previous example with equally spaced frequencies.

Both areas of the impedance spectrum could be covered also with a single multisine waveform. Properties of such signal with 12 frequency components are illustrated in Fig. 11.
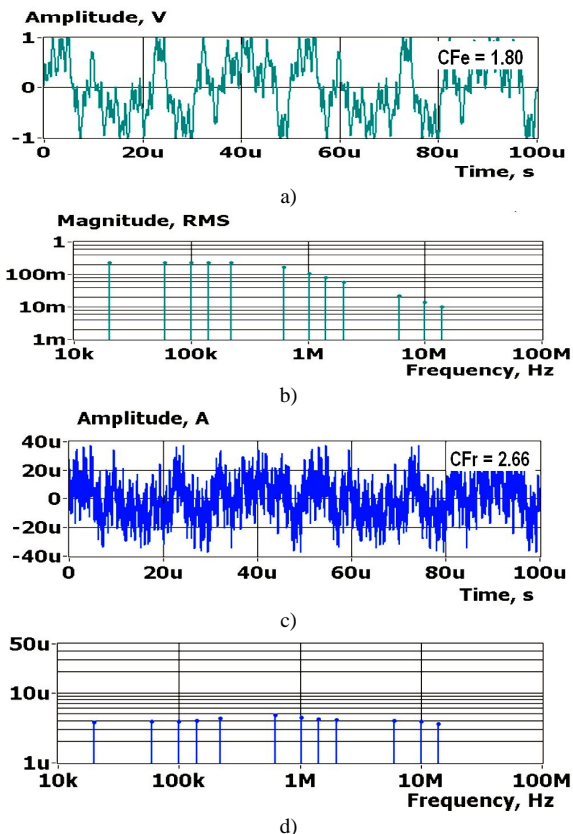
Fig. 11. Waveform of the voltage excitation (a) and it's spectrum (b), waveform of the response current (c), and it's spectrum (d). Ra = 1 , Ca = 2 pF and relative frequencies i = 1, 2, 3, 5, 7, 11, 31, 51, 71, 101, 301 and 501.

The first five frequency components of the excitation voltage are of constant amplitude 1V, and the amplitudes of next seven components are decaying as $V(i) = 1/i^{0.9}$. The product of the crest factors $CF_e \times CF_r$ = 5.0. It may be concluded on the basis of (7) that the SNR of impedance measurements with a single multisine excitation is less than in the case of using two separate multisine waveforms in the case of equal I_{max}.

VI. CONCLUSIONS

In general, the SNR of impedance measurement depends on the SNR of voltage and current measurements. If the amplitudes are limited, the crest factors of both signals are inversely proportional to the corresponding SNR.

The product of crest factors $CF_e \times CF_r$ can be used for rating the efficiency of excitation. At the same time, the product of crest factors depends also on the properties of electrical model and measurement circuit. It follows that the properties of the excitation signal and measurement mode (current or voltage excitation) should be adapted to the properties of the sample under test.

Use of the stable voltage excitation source and square waveforms eliminates the need for the excitation measurement and allows simple compensation of a decay of the typical bioimpedance spectrum in high frequency area. However, a frequency extent of the spectrum of square wave excitation signal should be strictly limited. Otherwise, the CF_r of the response current would be high (current peaks will appear), but removing of the trouble-making high frequency components complicates the measurement device.

An alternative solution is composing of near square wave excitation as a sum of sine waves (multisine waveform). Advantage of this solution is that only desired frequency components are present in the spectrum. Selection of amplitudes and optimal initial phases for the signal components allows designing of the multisine waveforms with significantly better efficiency compared to the binary square wave. As shown in the current paper, a multisine excitation with ten frequency components corresponding to the first ten components of binary square wave has similarly flat magnitude spectrum of the response current and near to 4 times smaller product of crest factors. It follows that, in this particular case, the SNR of measurements with a multisine excitation is also near to 4 times better.

The flat and decaying parts of the impedance magnitude spectrum could be covered with a single multisine excitation signal. In this case, the product of crest factors is nearly 5. However, a composite signal containing the separate part, which is designed only for measurement in the flat area of the spectrum, provides better results than a signal covering both regions of the impedance spectrum. A multisine with ten equally distributed relative frequencies i = 1, 2, 3, …, 10 gives the product of crest factors only 2, and a multisine with binary logarithmic distribution of relative frequencies i = 1, 2, 4, 8, 16, 32 provides the product of crest factors 4.2.

Complexity of generation and higher power consumption are the disadvantages of the multisine excitation in comparison with generating of binary multifrequency waveforms. Using of the binary waveforms is justified only if the above-mentioned disadvantages are crucial, as it is implantable and wearable devices.

REFERENCES

[1] S. Grimnes, O. G. Martinsen, *Bioimpedance and Bio-electricity Basics*. Elsevier-Academic Press, 2008, ch. 4–5.
[2] J. Ojarand, M. Min, "Simple and efficient excitation signals for fast impedance spectroscopy", *Elektronika ir Elektrotechnika*, no. 2, pp. 49–52, 2012. [Online]. Available: http://dx.doi.org/10.5755/j01. eee.19.2.3468
[3] J. Ojarand, M. Min, P. Annus, "Optimisation of multisine waveform for bio-impedance spectroscopy", *Journal of Physics: Conf. Series*, vol. 434, 2013, pp. 1–4. [Online]. Available: http://dx.doi.org/10.1088/1742-6596/434/1/012030
[4] J. Ojarand, M. Min, R. Land, "Comparison of spectrally sparse excitation signals for fast bioimpedance spectroscopy. In the context of cytometry", in *Proc. of IEEE Int. Symposium Medical Measurements and Applications (MeMeA)*, Budapest, 2012, pp. 1–5. [Online]. Available: http://dx.doi.org/10.1109/MeMeA.2012. 6226631
[5] M. Min, T. Parve, U. Pliquett, *Chapter: Impedance detection. In Encyclopedia of Microfluidics and Nanofluidics*. Springer, 2013, pp. 25. [Online]. Available: http://www.springerreference.com/docs/html/ chapterdbid/367827.html
[6] A. Di Biasio, L. Ambrosone, C. Cametti, "The dielectric behavior of nonspherical biological cell suspensions: an analytic approach", *Biophysical Journal*, vol. 99, pp. 163–174, 2010. [Online]. Available: http://dx.doi.org/10.1016%2Fj.bpj.2010.04.006
[7] M. Min, J. Ojarand, O. Martens, T. Paavle, R. Land, P. Annus et.al., "Binary signals in impedance spectroscopy", *Conf. Proc. IEEE Eng. Med. Biol. Soc.*, 2012, pp. 134–137. [Online]. Available: http://dx.doi.org/10.1109/EMBC.2012.6345889
[8] B. Sanchez, G. Vandersteen, R. Bragos, J. Schoukens, "Basics of broadband impedance spectroscopy using periodic excitations", *Meas. Sci. Technol.* vol. 23, pp. 1–19, 2012. [Online]. Available: http://dx.doi.org/10.1088/0957-0233/23/10/105501
[9] F. Malobertti, *Data Converters*. Dordrecht, The Netherlands: Springer, 2007, ch. 1.